

Investigation on $\text{Ag}_2\text{SO}_4\text{:La}_2(\text{SO}_4)_3$ binary system

K Singh, S W Anwane[†] & S S Bhoga*

Department of Physics, Amravati University, Amravati 444 602

[†]Department of Applied Physics, Ankush College of Engineering, Nagpur 440 017

*Department of Physics, Hislop College, Nagpur 440 001

Received 3 February 1999

The ionic conductivity of $(100-x)\text{Ag}_2\text{SO}_4\text{:}(x)\text{La}_2(\text{SO}_4)_3$ (where $x = 0$ to 60) system is investigated using complex impedance spectroscopy. The solid solubility limit up to 3.63 mole % of $\text{La}_2(\text{SO}_4)_3$ in room temperature orthorhombic $\beta\text{-Ag}_2\text{SO}_4$ is set with the help of X-ray powder diffraction, differential scanning calorimetry and scanning electron microscopy. The ionic transport number seen to remain invariant with SO_2 partial pressure. The major contribution to the conductivity within solid solubility limit is explained on the basis of presence of additional extrinsic vacancies. In bi-phase region, the 'optimum' dispersion of $\text{La}_2(\text{SO}_4)_3$ for $x=30$ provides conductivity enhancement by two orders of magnitude.

1 Introduction

Amongst sulphate based solid electrolytes, silver sulphate has potential application in electrochemical SO_2 gas sensors¹. It is the polymorphic compound which undergoes a phase transition from the high temperature highly conducting hexagonal α -phase to the low temperature moderately conducting orthorhombic β -phase at 416°C. As Ag^+ has low co-ordination number and high polarizability, it possess fast ion mobility².

In the specific applications like SO_2 gas sensors, the bi-phase solid electrolytes are more potential than single phase due to: (i) reduced porosity during sintering or volume changes which occurs by structural phase transition on heating/cooling³, (ii) moderate phase transition with low enthalpy⁴, (iii) improved electrode-electrolyte interface, (iv) exceptionally good long term chemical stability and (v) improved mechanical integrity^{5,6}.

The present work attempts a systematic study on variation of ionic conductivity on account of La^{3+} addition which influences Ag^+ mobility in both hexagonal (α) and orthorhombic (β) Ag_2SO_4 so as to understand the fundamental conduction processes and simultaneously to optimise material for SO_2 gas sensor.

2 Experimental Details

The initial ingredients Ag_2SO_4 and $\text{La}_2(\text{SO}_4)_3$ with assay more than 99.99% were procured from Aldrich Chemicals (USA). Pre-dried initial ingredients with mole fractions $(100-x)\text{Ag}_2\text{SO}_4\text{:}(x)\text{La}_2(\text{SO}_4)_3$ (where $x = 0.00, 0.5, 1.523, 2.565, 3.631, 4.73, 6.988, 8.166, 10, 20,$

30, 40, 50, 60) were mixed in an agate mortar under acetone for two hours. Silica translucent ampoules filled in with above mixture was heated in an electric furnace to the temperature 20°C above the melting point. Later, the melt was cooled slowly to room temperature with the cooling rate of 1.5°C/min. The ingot, obtained by breaking the ampoule was pulverized to obtain fine powder. The compositions with $x > 60$ mole % $\text{La}_2(\text{SO}_4)_3$ could not be prepared due to decomposition of Ag_2SO_4 at higher temperature.

The prepared samples were characterised by X-ray powder diffraction (XRD) (Philips PW 1700 diffractometer attached with PW 1710 controlling unit) using $\text{CuK}\alpha$ radiation. The micro-structures were examined with the help of scanning electron microscope (SEM) (Cambridge 250 Mark-III stereoscan electron microscope).

For electrical characterisation, the specimens were obtained in the form of circular discs (pellets) of 9 mm dia and 2 mm thick by uniaxially pressing the powder. Later the pellets were sintered at 500°C for 24 hr. Prior to spring loading of the pellets between silver electrodes, a good ohmic contact was ensured. Preceding to impedance measurement, the spring loaded samples were heated to 510°C for an hour in order to homogenize the charge carriers in the samples and simultaneously to remove the moisture content therein. The real and imaginary parts of the impedance were measured as a parametric function of applied frequency in the range from

5 Hz to 13 MHz and temperature from 510 to 100°C using hp 4192A Impedance analyser. The reproducibility of the impedance data was confirmed by repeating the measurement on the freshly prepared samples. The ionic transference number was measured by the Wagner's dc polarisation method using Keithley SMU 236 on cell Pt/Electrolyte/Ag.

3 Results and Discussion

A detailed analyses of results obtained towards the X-ray powder diffraction and scanning electron microscopy studies (as discussed elsewhere)^{7,8} suggest the formation of solid solution up to $x = 3.63$. Beyond this, they form two phase mixtures.

The variation of $\log \sigma$ with time (at fixed dc potential) shown in Fig. 1 reveals, in general, saturation to $\log \sigma_{\infty}$ after exponential decrease from zero time conductivity ($\log \sigma_0$). The ionic transference number is obtained using following Eq. (1)

$$\sigma_i = \frac{\sigma_0 - \sigma_{\infty}}{\sigma_0} \quad \dots(1)$$

It is worth mentioning here that the contribution of electronic part (σ_{elect}) to the total conductivity ($\sigma_T = \sigma_i + \sigma_{\text{elect}}$) is negligible and remains invariant over a wide range of SO_2 partial pressure. The above study indicates excellent chemical stability of electrolyte under test conditions.

Fig. 2 represents the complex impedance plot for (90) Ag_2SO_4 : (10) $\text{La}_2(\text{SO}_4)_3$. A closer look at the Fig. 2 reveals that the distorted semicircular arc is a combination of the two overlapping depressed semicircles (dotted one).

Since the conductive silver coating on both the surfaces of electrolyte acts as reversible (non-blocking) electrode, as expected, no polarisation reflects in the

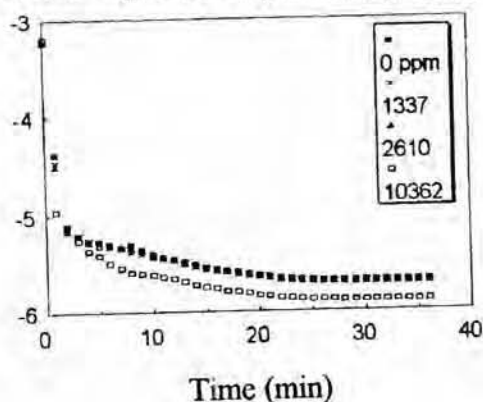


Fig. 1 — Variation of $\log \sigma$ with time after the application of 500 mV dc field

complex impedance plane. A non-linear least squares (NLS) fitting method is used to ascertain the presence of two overlapping depressed semicircular arcs and subsequent analysis. In order to accomplish it, the complex impedance data is fitted to equation:

$$Z(\omega) = R_0 + \frac{R_{b1}}{1 + (j\omega\tau^*_{1})^{\alpha_1}} + \frac{R_{b2}}{1 + (j\omega\tau^*_{2})^{\alpha_2}} \quad \dots(2)$$

where, R_{b1} and R_{b2} are due to first and second semicircles respectively; τ^*_{1} and τ^*_{2} are the mean relaxation times. During the NLS fitting the sum of squares of residuals of real and imaginary parts is minimised by unity weighting using our software developed in turbo C. Identical approach has been adopted earlier to ascribe the presence of two semicircles in the complex impedance plane^{7,9}. The presence of two overlapping depressed semicircular arcs suggests the occurrence of two prominent conduction mechanisms simultaneously under the external perturbation ac signal.

In case of polycrystalline bi-phase electrolytes, conduction through interface (space charge layer) of grains plays very important role. Two major interfaces taking part in the conduction are $\text{Li}_2\text{SO}_4/\text{Li}_2\text{SO}_4$ (MX/MX)-homo-junction and $\text{Li}_2\text{SO}_4/\text{La}_2(\text{SO}_4)_3$ (MX/M'X)-hetero-junction¹¹.

In Li_2SO_4 single phase, in concurrence with the space charge theory, an interfacial surface reaction at homo-junction increases interstitial Li^+ concentration adjacent to the surface of one grain and equivalent Li^+ vacancy concentration adjacent to the surface of other grain in contact¹². The surface interaction at $\text{Li}_2\text{CO}_3/\text{La}_2(\text{SO}_4)_3$ -hetero-junction could be analogous to that described earlier¹¹. Obviously, the defect concentration in the homo- and hetero-junctions differs considerably resulting into a large difference in ion mobility, jump frequency and activation energy. All these factors are

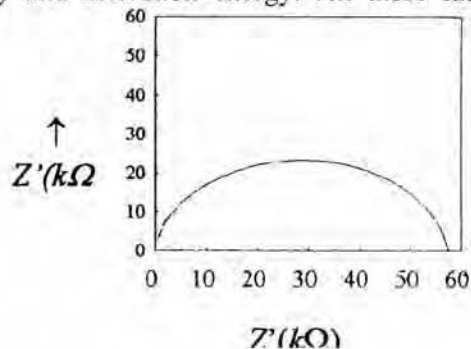


Fig. 2 — Impedance plots for (90) Ag_2SO_4 : (10) $\text{La}_2(\text{SO}_4)_3$

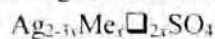
responsible for two semicircular arcs in the complex impedance plane. Maier has also predicted two distinct hopping rates in the space charge regions due to homo- and hetero-junctions¹³. In any electrochemical devices, the total conductivity of electrolyte is of importance, hence, it was determined from the real axis intercept of the complex impedance plot (R_{b2}). Conductivity obtained following complex impedance analysis excludes contribution from polarisation and electrode/electrolyte interface effects.

Over the entire temperature range of investigation, the conductivity (σ) of all the compositions obeyed the Arrhenius equation:

$$(\sigma T) = (\sigma T)_0 \exp(-E_a/kT) \quad \dots(3)$$

The variation of conductivity at 505°C with concentration x , depicted in Fig. 3, reveals two maxima. The first maximum at $x = 3.63$ lies within the solid solubility region, whereas, the second one at $x = 30$ belongs to bi-phase region. The maximum conductivity in these regions is as follows:

Region I: The ionic conductivity within the solid solubility limit initially enhances with $\text{La}_2(\text{SO}_4)_3$ content and optimises nearly at 6.988 mole%. Beyond this concentration it decreases. The partial replacement of host monovalent by guest trivalent ions gives rise two additional extrinsic vacancies in the host lattice conforming to the formula;



Also, mobile Ag ions squeeze through the lattice with an elementary hopping to the extrinsic vacancies in the close vicinity of the impurity (La^{3+}) as lattice experiences local strain⁹. Further addition of $\text{La}_2(\text{SO}_4)_3$, for $x > 3.63$ (i.e., beyond 7 vacancy %) the conductivity decreases following vacancy-vacancy interactions such as cluster formation and also cationic sublattice ordering¹⁰. These opposite effects cancel each other at conductivity maximum for $x = 3.63$.

Region II: In bi-phase region, $4.72 < x < 60$, the conductivity increases with the increase in the $\text{La}_2(\text{SO}_4)_3$ content with maximum at $x = 30$ mole % followed by the decrease (Fig. 3). A conductivity enhancement in a binary system can be caused by the presence of an intermediate phase which has conductivity higher than those of pure components. However, this possibility is ruled out (on the basis of X-ray powder diffraction results) in the present system.

The major contributions to the total conductivity of present bi-phase system is from (i) Li_2SO_4 solid solution (ii) $\text{La}_2(\text{SO}_4)_3$, (iii) homo-junction (interface between

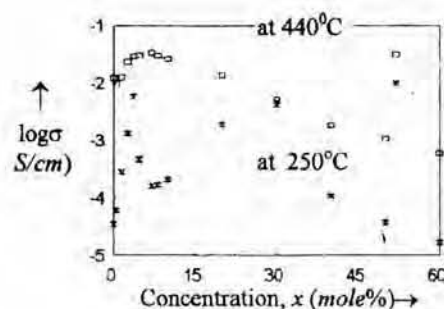


Fig. 3 — Variation of $\log \sigma$ with $\text{La}_2(\text{SO}_4)_3$ concentration

$\text{Li}_2\text{SO}_4/\text{Li}_2\text{SO}_4$) and (iv) hetero-junction (interface between $\text{Li}_2\text{SO}_4/\text{La}_2(\text{SO}_4)_3$). Since total conductivity of the samples of this region is higher than that of the individual phases, hetero-junction chiefly contributes to an enhancement in conductivity.

As the concentration of second phase increases, the insoluble phase precipitates out and subsequently disperses into Ag_2SO_4 (solid solution) matrix. Such dispersion increases highly conducting hetero-junctions forming more ion percolating paths thereby increases the conductivity. The maximum conductivity at $x = 30$ is due to the percolation threshold concentration. The decrease in σ beyond percolation threshold is attributed to the disruption of percolation paths due to agglomeration of grains.

4 Conclusion

Partial substitution of aliovalent La^{3+} for Ag^+ enhances the conductivity via vacancy mechanism. Whereas, in the bi-phase region highly conducting surface percolating paths (hetero-junction) plays important role. Highest conducting binary system may be used in electrochemical applications especially SO_2 sensors.

Acknowledgement

Authors are thankful to the Department of Science and Technology, New Delhi (No. III(4-42)93-ET) for providing financial assistance to carry out this work.

References

- 1 Liu Q G & Worrell W L, *US Patent Applic.*, 17 (1981) 303
- 2 Cotton F A & Wilkinson G, *Inorg Chem.*, (1966) 894
- 3 Saito Y, Maruyama T, Matsumoto Y & Yano Y, *Proc Int Meet Chem Sensors*, Vol. 17, Anal Chem Symp Series. (Elsevier, New York) 1983, 326.
- 4 Rao N & Schoonman J, *Solid State Ionics*, 57 (1992) 159.
- 5 Worrell W L & Liu Q G, *J Electroanal Chem.*, 168 (1984) 355.
- 6 Liu Q G & Worrell W L, *Solid State Ionics*, 18 & 19 (1986) 524.

- 7 Singh K, Pande S M, Anwane S W & Bhoga S S, *J Appl Phys*, (In press) (1998).
- 8 Singh K, Anwane S W & Bhoga S S, *Solid State Ionics*, 86 (1996) 187.
- 9 Singh K, Pande S M, Anwane S W & Bhoga S S, *Bull Electrochem*, (1996).
- 10 Hofer H H, Eysel W & Alpen U V, *J Solid State Chem*, 36 (1981) 365.
- 11 Singh K, Pande S M & Bhoga S S, *J Solid State Chem*, 116 (1995) 232.
- 12 Maier J, *Ber Bunsenges Physik Chem*, 90 (1986) 29.
- 13 Maier J, *Solid St Ionics*, 75 (1995) 139.